Heterogeneous glass transition behavior of Poly(ethylene oxide)/Silica nanocomposites via atomistic MD simulations

Ioannis Tanis[1], Albert J. Power[2,3], Antonis Chazirakis[2,3] and Vangelis Harmandaris[1,2,3]**

[1]Computation-based Science and Technology Research Center, The Cyprus Institute, 2121 Nicosia, Cyprus

[2]Department of Mathematics & Applied Mathematics, University of Crete, 70013 Heraklion Crete, Greece

[3]Institute of Applied and Computational Mathematics, Foundation of Research and Technology-Hellas, 700 13 Heraklion, Greece

Abstract. Adding nanofillers in polymer matrices results in a slowing down of the polymer dynamics, for attractive polymer/nanofiller interactions. In this work, we perform atomistic molecular dynamics simulations in poly(ethylene oxide)/silica model nanocomposites to investigate the, spatial heterogeneous, glass transition behaviour of the polymer chains. To address this, we compute both the "thermodynamic" and the "dynamic" glass transition temperature of polymer chains, as a function of the silica loading. The "dynamic" glass transition within specific domains is estimated via a novel method, based on the translational dynamics of the polymer monomers. A clear increase of the glass transition temperature of polymer chains with nanoparticles loading is found. In addition, a spatial gradient in the glass transition behaviour is identified, in agreement with experimental studies in polymer nanocomposites with attractive polymer/nanofiller interactions. The local dynamical heterogeneities of polymer chains in the nanocomposites are further examined via a geometric analysis, by probing the evolution of the "slow" polymer regions, as temperature decreases. The "onset" of the glassy state, defined by the percolation of the slow regions, is found in qualitative agreement to the thermodynamic and dynamic approaches.

1.Introduction.

The dispersion of nanofillers into a polymer matrix is known to induce profound changes to the bulk properties such as the melt viscosity and the glass transition temperature (T_g).[1, 2] These changes are both due to geometrical confinement (entropic effect), as well as to the modification of the segmental dynamics in the presence of the fillers due to the enthalpic polymer/solid interactions.[3-7]

Indeed, it has been demonstrated by experimental and simulation studies that attractive interfacial interactions tend to slow down the relaxation modes of the polymers at the interface, thus resulting in a shift of the polymer T_g [8-11] . On the other hand, other works suggest that the restriction of chain mobility caused by the nanoparticles, does not extend throughout the matrix but affects only the chains within a few nanometers of the nanoparticle surface, also known as the bound layer.[4, 9] Moreover, few studies have further examined heterogeneities, such as spatial gradients, regarding glass transition properties in polymer nanocomposites (PNCs).[12, 13] For example, recently, Wei and Torkelson conducted fluorescence studies in PNCs in order to assess the changes in the average bulk T_g and near-interface alterations in T_g, as functions of poly(2-vinylpyridine) (P2VP) molecular weight (Mw) and silica content.[11] Their findings revealed a sharp increase in bulk T_g for high Mw PNCs with increasing silica content, whereas moderate changes in T_g were observed for lower Mw matrices. Papon and co-workers proposed that the T_g of model nanocomposites composed of a poly(ethyl acrylate) matrix with grafted monodispersed silica particles of varying diameters, varies with the distance from the nanoparticle (NP) surface via an empirical relation.[3] Chakraborty and co-workers employed coarse-grained MD simulations to examine the effect of polymer-filler interactions on the T_g of a poly(vinyl alcohol) (PVA)/silica nanocomposite. [8] Their findings demonstrated that by tuning the number and the strength of specific hydrogen bonds enables to optimize the T_g of the nanocomposite system targeted for specific applications. [8] Another study of Pavlov *et al.* reported an increase in the T_g of crosslinked polybutadiene rubbers when added with silica NPs, even at low loadings i.e. (at weight functions equal to 10%). [14] Despite the fact that the thermodynamic, and dynamic T_g in confined polymer-based materials has been studied before via simulation approaches[15-17], to our knowledge, there are no studies of polymer/SiO_2 nanocomposite systems, via detailed atomistic simulations. The latter are necessary in order to describe local phenomena in the sub-nanometer scale, such as, for example, the density heterogeneities at the polymer/nanofiller interphase which occur within distances less than one 1 nm from the nanoparticle (silica) surface, and, consequently, cannot be captured by generic bead spring models, in which the bead size is of the order of a Kuhn segment. Furthermore, atomistically-detailed models can additionally describe specific interactions, such as the hydrogen bonds, due to which attractive polymer/nanoparticle interactions appear. [18, 19]

In the present work, we investigate the spatial heterogeneous glass transition in PNCs of varying nanoparticle content, at the atomic scale, bearing attractive polymer/filler interactions. We further predict the temperature dependence of the polymer segmental dynamics and explore the relation between the thermodynamic and dynamic T_g estimations[20, 21], focusing on the

polymer/filler interface. As a model polymer nanocomposite system of attractive polymer/filler interaction, we study poly(ethylene oxide)/silica, PEO/SiO_2, PNC, the structural and dynamic properties of which have been thoroughly examined by both experimental[22-25] and numerical[26-29] approaches, the latter conducted primarily in the melt regime though.

2.Model and Simulation Method.

We consider a polymer matrix comprising 50-mer PEO chains, terminated with methyl groups. The silica nanoparticle embedded in the polymer matrix is of approximately spherical shape of radius ∼2 nm. A detailed description of the examined systems is provided in Table 1. We stress here that our simulation model systems assume a good dispersion of the nanoparticles in a cubic arrangement induced by the periodic boundary conditions.[24] As the major goal of our work is the examination of confinement effects on the local glass transition temperature, as well as the system's heterogeneous dynamical behaviour, retaining similar, well dispersed nanoparticle conditions, ensures a trustworthy comparison among system of different NP volume fraction. We also stress here, that, as the majority of the systems correspond to the diluted regime, the results should not be significantly affected by the regular spacing between the nanoparticles. All MD simulations were conducted with the aid of GROMACS software. [30]

Details of the simulation model and the equilibration protocol are given elsewhere [31]. Initial atomistic PEO/SiO_2 configurations at a high temperature (T = 400K) were obtained from a previous work. [31] The models were afterwards subjected to MD cooling steps of 10K in the isobaric-isothermal ensemble down to T = 150K. For each of the investigated systems, cooling was performed for 3 uncorrelated configurations to improve statistics. At each cooling step, MD runs of 10 ns were performed, after the first 5 ns of which the potential energy and the specific volume of the system were stabilized.

Hybrids	w_{SiO2}[a] (wt)	φ_{SiO2}[b] (vol)	ID[c] (nm)	ID/2R_g[d]
Hybrid_1	5.05	1.9	11.809	3.31
Hybrid_2	11.98	4.5	8.74	2.45
Hybrid_3	19.98	7.6	7.24	2.03
Hybrid_4	33.3	12.7	5.92	1.66
Hybrid_5	42.07	16.1	5.33	1.49
Hybrid_6	49.97	19.1	4.93	1.38

Hybrid_7	57.1	21.8	4.62	1.29

[a]w_{SiO2} : weight fraction of the silica nanoparticle

[b]φ_{SiO2} : volume fraction of the silica nanoparticle

[c]ID : the nearest interparticle distance

[d]ID/R_g : the degree of chain confinement (R_g is the radius of gyration of the bulk PEO 50-mer)

Table 1: Details of the simulated PEO_{50}/SiO_2 nanocomposites.

3.Thermodynamic and Dynamic T_g calculations.

Initially, we examine the glass transition of the overall confined system by computing the T_g via both thermodynamic and dynamic criteria. The standard thermodynamic method relies in computing the change in slope of the temperature dependence of the specific volume of the polymer chains, as shown in Figure 1 for three indicative systems.

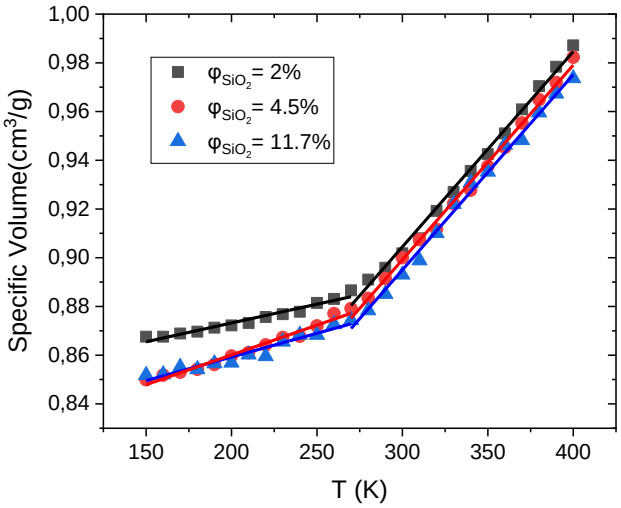

Figure 1: Specific volume as a function of temperature as determined from the NPT runs for three filler volume fractions φ_{SiO2} = 2, 4.5 and 11.7%.

The dynamic glass transition temperature is typically obtained via probing the segmental relaxation autocorrelation functions, as for example in dielectric spectroscopy measurements, and defining an arbitrary timescale; usually dynamic T_g is the temperature in which the segmental relaxation time becomes ≈100sec. However, such timescales are inaccessible by atomistic MD simulations. Alternatively, in case dielectric spectroscopy measurements at lower temperatures were available, experimental data could be used together with the high temperature MD data to provide a study across a broad range of temperatures.[32] In this work,

we use a criterion that is based on the segmental translational dynamics by probing the mean square monomer displacement of polymer chains, $\Delta R^2(t)$, as a function of time for the different systems. This approach is very similar to the calculation of the T_g via the temperature dependence of the dynamic structure factor as obtained by incoherent elastic scattering experiments.[33, 34] Indeed, since our approach uses the MSD to probe the glass transition of the PEO chains, our results shouldn't differ from the calculation of the dynamic structure factor as, in the Gaussian approximmation, the latter relates directly to the MSD.[34] Furthermore, as it is well known, the relaxation times can reach hundreds of nanoseconds upon approaching the glassy regime[35], our method is significantly faster and computationally less demanding, as the trajectories used for the dynamic analysis were of length equal to10 ns. A visual inspection of the time dependence of the mean-squared displacement of the chain monomers illustrated in Figure 2b for the neat polymer model, reveals a characteristic timescale of the order of 1 ps which corresponds to a "caging" time, t_c, when local translational motions are frozen in the glassy state. [36-38] We can also detect a longer timescale t^*, of the order of approximately 100-200 ps, at which, due to the caging effect, the monomer $\Delta R^2(t)$ tend to reach a constant value, i.e., the first derivative of the $\Delta R^2(t)$ with respect to time exhibits a sharp decline. The temperature at which a sudden drop of $d(\Delta R^2(t))_{t=t*}/dt$ is detected, defines the onset of the glassy state. Here we use t^*=200ps but in practice any choice between 100 -1000 ps should yield very similar results. To verify that this is the case, we have conducted analogous calculations at t^*=1000ps for the system at φ_{SiO2} = 4.5%. Results at both t^* values (not shown) yield that this system reaches the glassy state at a temperature near T = 290K. The corresponding data for t^*=200ps are illustrated for all examined systems, in Figure 2c.

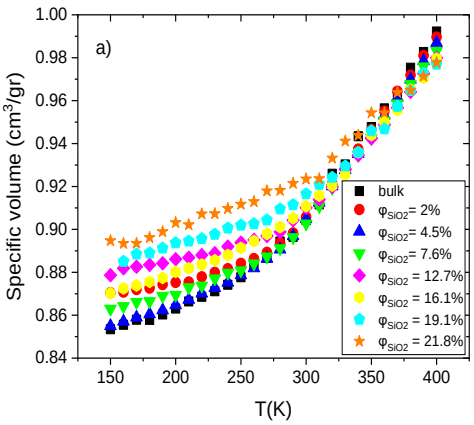

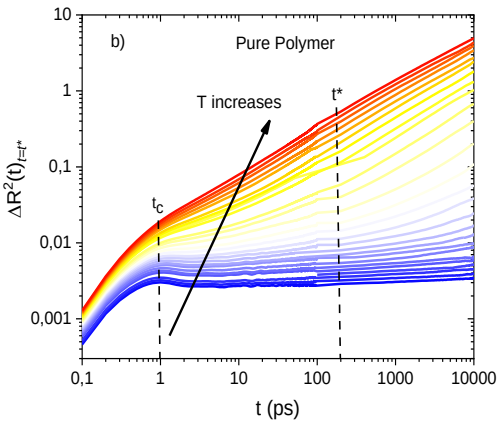

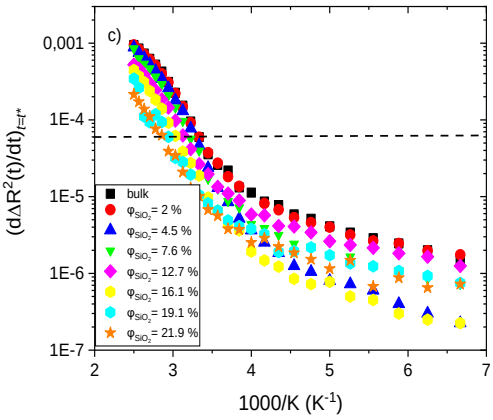

Figure 2: a) Specific volume as a function of temperature as determined from the NPT runs for bulk polymer and PEO/SiO_2 model systems. b) Time dependence of the mean-squared displacement of the polymer chain monomers in the bulk, $\Delta R^2(t)$. *t** refers to the timescale at which the calculations of $d(\Delta R^2(t))/dt$ are performed, whereas t_c refers to the onset of caging. c) Time derivative of $\Delta R^2(t)$ of the chain monomers, at *t**, as a function of the inverse temperature. The dashed line perpendicular to the y-axis denotes approximately the transition from the glassy to the melt state. Data are shown in the temperature range 150-400K.

Data regarding the temperature dependence of the specific volume and the segmental (monomer) dynamics of polymer chains, for all model PEO/SiO_2 systems, as well as of bulk PEO, are shown in Figure 2. A visual inspection of Fig.2a reveals that the change in slope of the specific volume curve is shifted to higher temperatures as filler concentration rises. This lies in agreement with experimental and simulation studies reporting an increase of the T_g of a polymer matrix embedded with nanoparticle fillers interacting favourably with the polymer chains, is elevated with respect to the T_g of the pure polymer. [8, 9] Focusing on Fig.2c, a rapid drop of $d(\Delta R^2)_{t=t*}/dt$ is observed at high temperatures, followed by less abrupt changes as temperature decreases. $d(\Delta R^2)_{t=t*}/dt$ reaches values smaller than 1E-06 at the lowest examined temperature. This is expected as no diffusive motion is detected at this temperature regime.

The critical value of $d(\Delta R^2)_{t=t*}/dt$ after which the polymer matrix exhibits a glassy-like behavior, is defined as the value corresponding to the thermodynamic glass transition temperature of the pure polymer. Examining Fig.2a, we can discern that, for the pure system, this derivative at the intersection temperature (T = 270K) of the melt and glass thermal expansion curves, reaches the value $d(\Delta R^2)_{t=t*}/dt \cong 5 \times 10^{-5}$. Therefore, reaching this value can be taken as a dynamic calculation of the glass transition temperature. On these

grounds, we define the dynamic T_g of all systems as the temperature where $d(\Delta R^2)_{t=t*}/dt \cong 5 \times 10^{-5}$ in order that the value extracted from the dynamic analysis is equal to the thermodynamic value for the bulk PEO model.

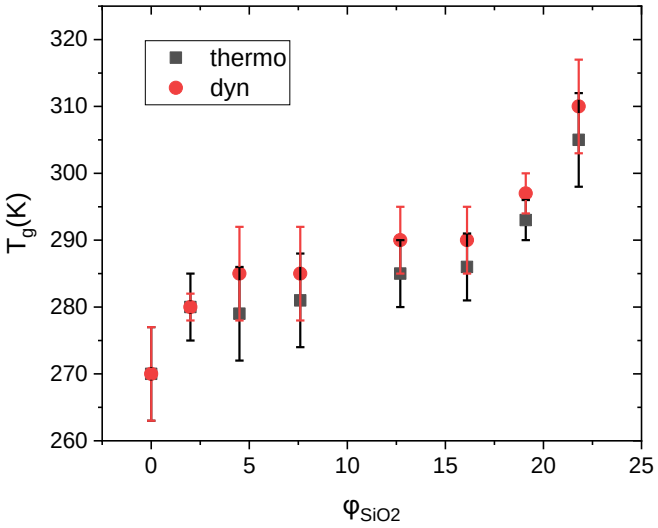

Figure 3: Estimated glass transition temperature of PEO chains in PEO/SiO_2 model nanocomposites as determined by both the thermodynamic, "thermo", and dynamic, "dyn", approaches, as a function of silica loading.

Figure 3 presents the polymer glass transition temperature as estimated from both the thermodynamic and the dynamic methods explained above. The T_g data presented in Fig. 3 as extracted from both the thermodynamic and dynamic approach, demonstrate a non-linear increase in the polymer T_g as filler content rises. The polymer T_g is elevated by approximately 15K for filler content up to 16%, whereas more pronounced changes are observed at higher silica concentrations. Dynamic glass transition values are in reasonable agreement with the thermodynamic data at all silica loadings. Experimental data on the T_g of PEO report a T_g value of 206K for high molecular weight PEO bulk system.[39] Such differences between simulation and experimental data on glass transition temperature of glass-forming liquids are not surprising considering the much different cooling rate used in the two different approaches. Indeed, simulations use a very rapid cooling rate of the order of 1K/ns, as the one used here (that is lower than typical cooling rates reported in simulation literature[39]), compared to the experimental quenching rate that is about 1K/sec.[38] Given the semi-empirical observation that the T_g is affected strongly by the cooling rate with about 3-5 degrees per decade we expect differences between 30-50 K.[38] Other factors that trigger deviations between the experimental

and simulation values, are the polydispersity of the actual sample and the possible existence of residual solvent used in the preparation procedure that could lower the experimentally measured T_g .[40]

To examine whether a near-interface spatial gradient in T_g exists, we estimated the resolution of the average T_g to its near-interphase T_g ($T_{g,inter}$) and average matrix T_g ($T_{g,matrix}$) with the aid of the thermodynamic and dynamic methods described earlier. In order to identify the adsorbed layer region, the mass monomer radial density profile of the PEO chains as a function of the nanoparticle center of mass, was calculated.

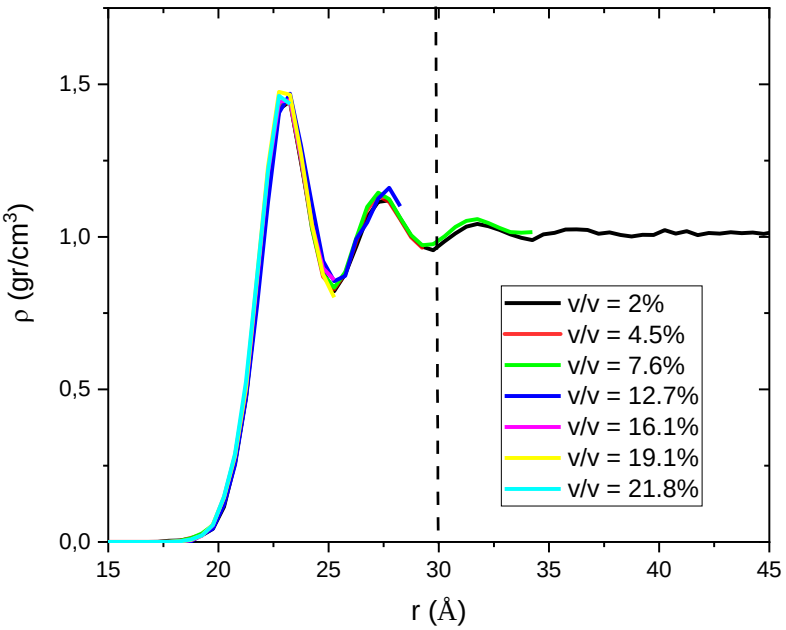

Figure 4 : Mass monomer density profiles of the PEO chains with respect to the center of mass of the SiO_2 nanoparticle for different filler volume fractions at T = 400K. The dashed line defines the border between the interphase and the matrix polymer regions.

The chains that reside at a distance less or equal to the minimum of the second peak of the monomer density profile were considered to belong to the interphase region whereas those residing at larger distances were included in the matrix region. A visual inspection of Fig.4 reveals that, at filler concentrations higher than 7.6%, the matrix region does not exist. On these grounds, the layer-resolved calculations of the glass transition temperature were performed at filler concentrations of 2%, 4.5% and 7.6%. The corresponding graphs are illustrated in Figure 5.

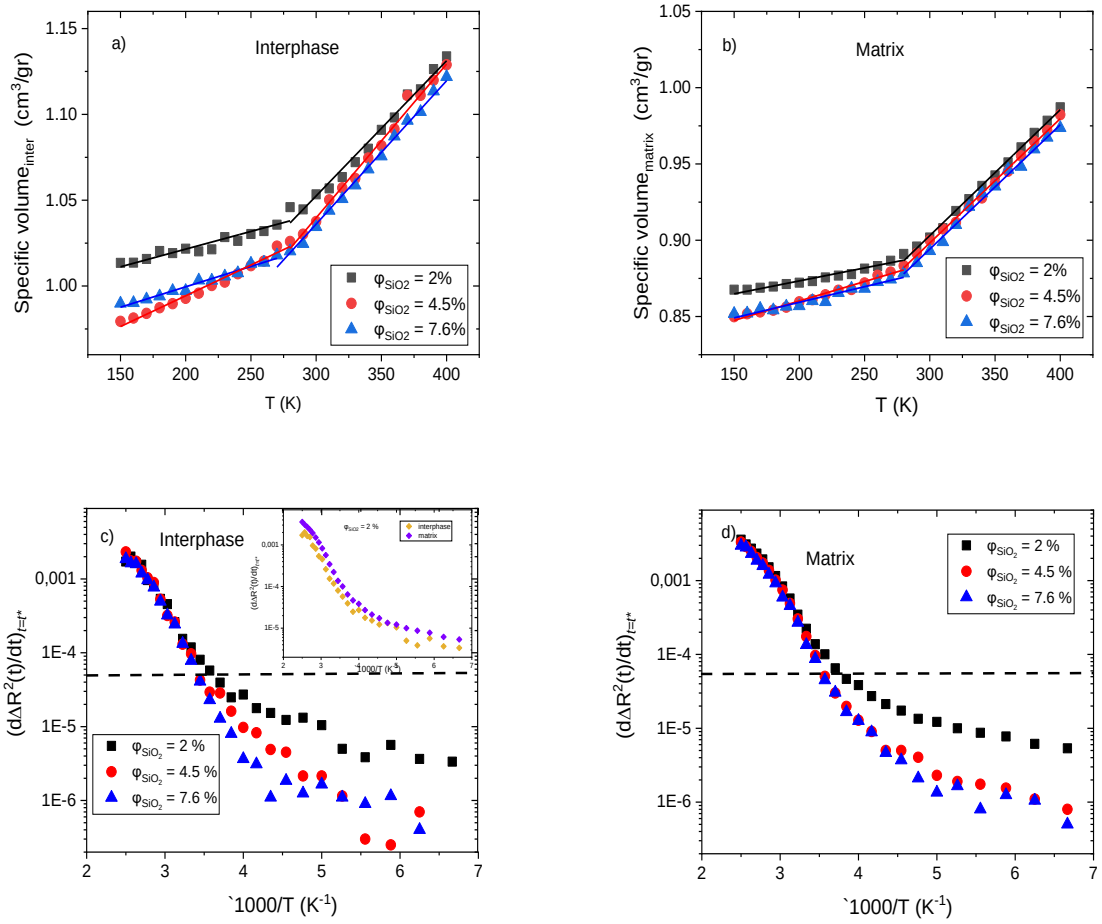

Figure 5: Top panel: Specific volume as a function of temperature as determined from the NPT runs for the a) interphase and b) matrix regions. Bottom panel: Time derivative of the $\Delta R^2(t)$ of the chain monomers, at t^*, as a function of the inverse temperature for the c) interphase and d) matrix region. The dashed line perpendicular to the y-axis denotes the transition from the glassy to the melt state. The inset figure in c) displays the time derivative of $\Delta R^2(t)$ at the interphase and matrix regions for the system with filler content 2%.

As it can be inferred from the top panels of Fig.5, the interphase region, despite the thin dense layer, is characterized by an average slightly lower density, compared to the matrix. This is due to the excluded volume interactions of the SiO_2 atoms, and of the adsorbed PEO ones as well, and has been also reported for glassy PEO/SiO_2 model systems.[41] On the other hand, a visual inspection of the inset figure 5c shows the existence of slightly higher mobility gradients at the matrix region, which are consistent to the absence of polymer-filler interactions at this region. Similar to the T_g calculations presented in Fig. 3, the T_g values of

the interphase and matrix region, were extracted, based on both thermodynamic and dynamic criteria and are listed in Table 2.

System	$T_{g,inter,\ thermo}$	$T_{g,inter,\ dyn}$	$T_{g,matrix,\ thermo}$	$T_{g,matrix,\ dyn}$
2%	281±10	285±21	274±8	270±14
4.5%	279±8	295±21	274±3.5	280±15
7.6%	282±6	295±21	277±3.5	285±15

Table 2: Layer-resolved calculation of the glass transition temperature of PEO via the thermodynamic and dynamic approaches.

Examining the data in Table 2, we observe that the PEO $T_{g,inter}$ values are consistently higher than those at the matrix region. This lies in accordance with the findings of Wei and Torkelson who carried out a similar analysis in P2VP/Silica nanocomposites via fluorescence spectroscopy.[11] In a manner similar to the discussion of that work, the differences between $T_{g,inter}$ and $T_{g,matrix}$ can be ascribed to dispersive and hydrogen bonding interactions between the ether oxygen atoms in PEO and the silanol and hydroxyl groups on the silica surface.
Similar to the average T_g data presented in Fig. 3, the local T_g rises mildly for nanofiller concentration up to 7.6%. Contrary to our findings, Wei and Torkelson report large alterations for the near-interface T_g for the P2VP/Silica nanocomposite, even at low filler loadings[11]. This discrepancy might be attributed to the stronger polymer-filler interactions at the P2VP/SiO_2 system compared to the PEO/SiO_2 one. A comparison between the 'thermo' and 'dyn' values of Table 2, shows, similarly to Fig.3, that the latter are consistently higher than their 'thermo' counterparts.

4. Effects of spatial gradient in T_g on the segmental dynamics.

To examine how the spatial gradient in T_g affects the segmental dynamics of the polymer chains, a layer-resolved analysis of the monomer $\Delta R^2(t)$s was performed. Figure 6 presents the temperature and temporal dependence of the monomer $\Delta R^2(t)$s at the different layers at times t =200ps and t = 5000ps.

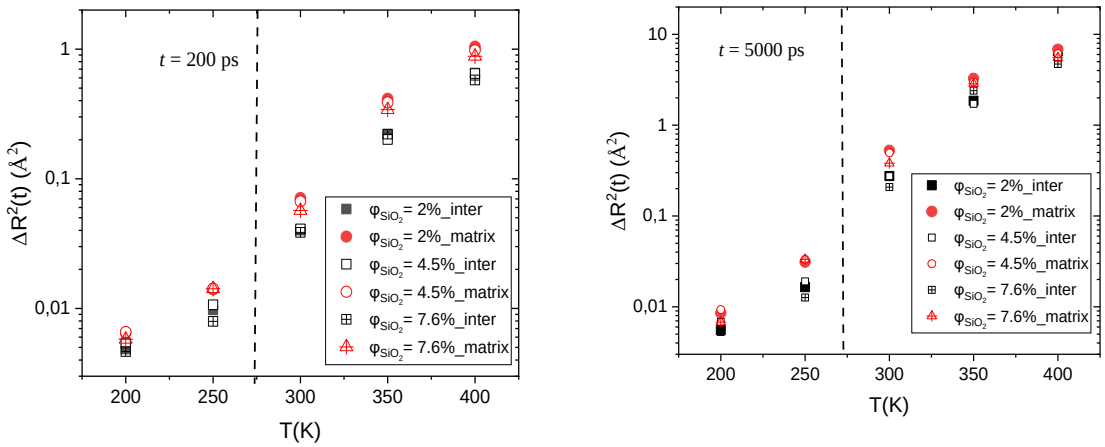

Figure 6: Layer-resolved calculation of the PEO monomers' mean-squared displacements. Results are presented as a function of temperature at timescales of a) t=200ps and b) t=5000ps. The dashed lines perpendicular to the x-axis denote approximately the transition from the glassy to the melt state in the bulk PEO model systems.

As it can be inferred from Fig. 6, a significant increase in $\Delta R^2(t)$ is observed at $T > T_g$ at all times due to the activation of the α-process as well as other segmental motions.[41] As expected, the polymer chains belonging to the matrix region are more mobile than their counterparts residing at the interphase region. The system bearing the lowest filler concentration appears to be the most mobile. This is probably due to the fact that the matrix region in this model is much larger than the interphase region as compared to the other systems.

Comparing the monomeric $\Delta R^2(t)$s shown in Fig.6a, we observe that, at short times, the differences in mobility among systems of different filler content are more pronounced at elevated temperatures (T > 300K), well above the T_g. A similar trend is observed when comparing the layer-resolved $\Delta R^2(t)$s. This is not the case at longer times since the differences in mobility among the PNC models become larger upon cooling. On the other hand, focusing on the $\Delta R^2(t)$ values at high temperatures, minor differences are detected between the inter and matrix regions. This behaviour implies that dynamic heterogeneities tend to disappear upon heating the system well above its T_g. This trend lies in accordance with findings from other experimental and simulation studies in thin polymer films and binary Lennard-Jones liquids.[43-48]

To obtain a visual inspection of the dynamically heterogeneous regions of the models, a 3D decomposition of the simulation box in sub-cells of size of 5Å each, was performed. The average monomer mean square displacement $\Delta R^2(t)$ at t^* =200 ps was calculated and each

subcell was classified as “fast”(or “slow”) according to whether its average $\Delta R^2(t)$ was larger (smaller) than the average pure PEO monomer at the model T_g, i.e. $\Delta R^2(t*)_{T=T_g} = 0.0375 Å^2$. Then, we derive a 3-dimensional distribution (heat -like map) of the ‘slow’ subcells around the silica nanoparticle for each system at a given temperature. Representative distributions are illustrated in Figure 7. A clear percolation of the “slow” regions, as the temperature decreases, is observed.

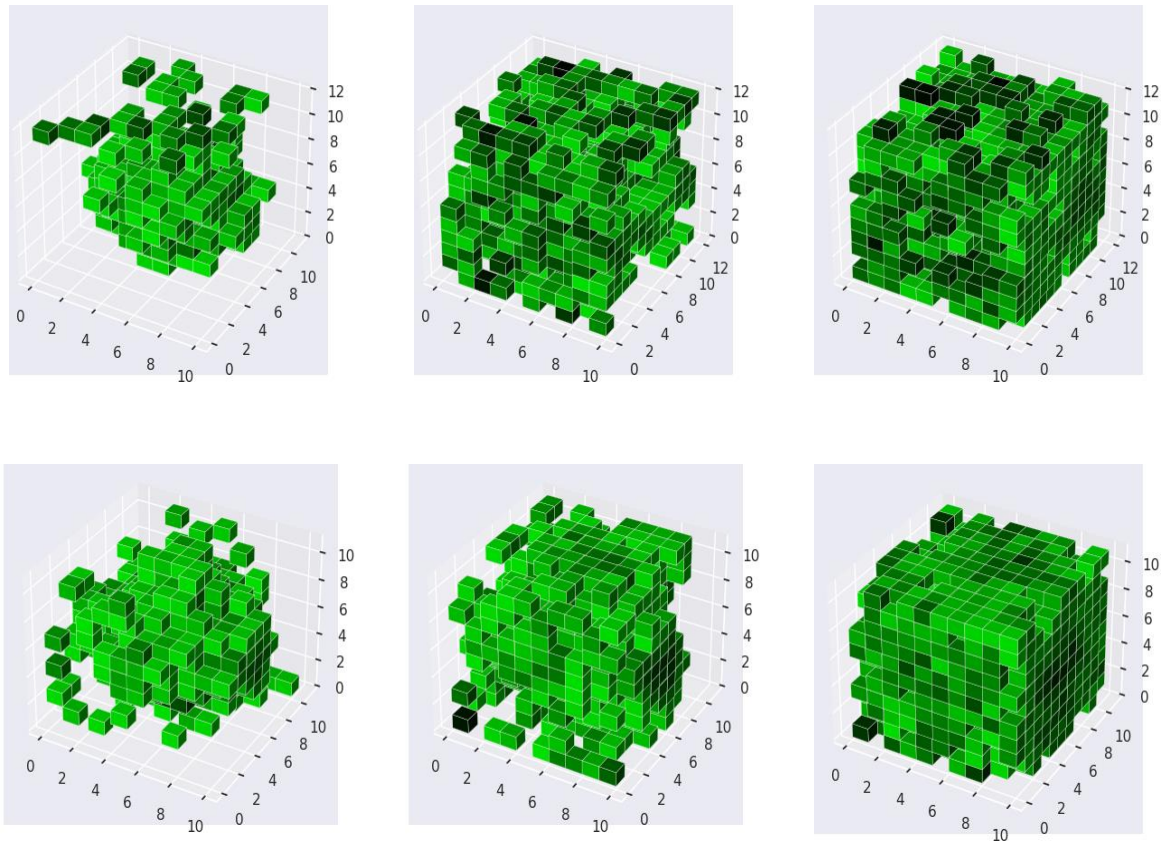

T = 320K T = 310K T = 300K

Figure 7: 3-dimensional distributions of the subcells defined as ‘slow’, i.e. the subcells where the average monomer $\Delta R^2(t) < 0.0375$ A^2, at $t = t^*$ for the system of φ_{SiO2} = 12.7% (top) and the system of φ_{SiO2} = 16% (bottom). The NP is omitted for clarity.

To quantify the above percolation threshold, we present in Figure 8 the percentage of slow monomers as a function of temperature for all examined model PEO/SiO_2 systems. It is clear that the percentage of slow monomers (%PSM) drops slower as the volume fraction of the

nanofiller rises. This lies in accordance with the results from Fig.6 demonstrating a higher mobility for the lower filler content systems. We can also identify a temperature at which a sudden drop of %PSM is detected, so we can surmise that this temperature corresponds to the onset of the glassy state. The extracted T_g's are listed in Table 3 and lie in qualitative agreement with the "thermo" and "dyn" T_g data presented in Figure 3. We also note that, as the data derived from the percolation analysis are prone to quenching effects as the results presented in Fig.3 and Table 2, the glass transition temperatures are larger than the experimental ones.

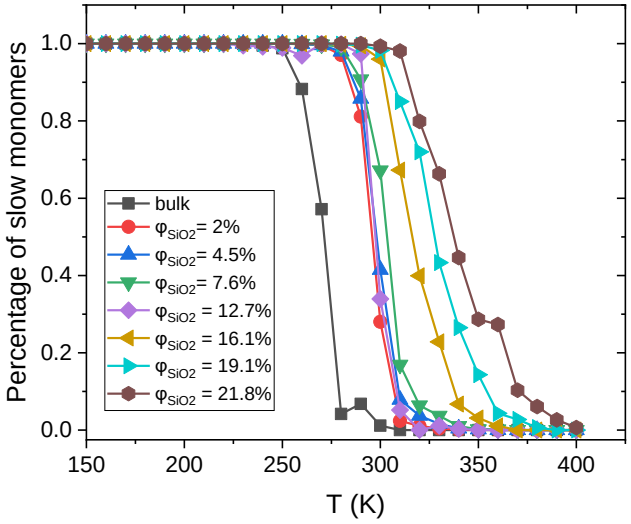

Figure 8: Fraction of chain monomers identified as 'slow' (see main text) as a function of temperature for all filler contents.

System	T_g, (K)
Pure	260±7
2%	290±7
4.5%	290±5
7.6%	290±4
12.7%	290±4
16.1%	300±7
19.1%	320±5
21.8%	330±5

Table 3: Estimated glass transition temperature of PEO determined as the temperature at which a sudden drop of the percentage of slow monomers is observed.

5. Conclusions.

Overall, we proposed an investigation, at the atomic level, of the heterogeneous glass transition behaviour of polymer chains in PEO/SiO_2 nanocomposites. Data were presented as a function of the nanofiller content in order to examine the alterations in T_g associated with the polymer confinement and the polymer-filler interactions. The glass transition temperature of the nanocomposite models was estimated via both thermodynamic and dynamic approaches, the results of which were found to lie in satisfactory agreement. Layer-resolved calculations of the glass transition temperature exhibit spatial gradients in T_g, in agreement with recent experimental findings in nanocomposites with attractive polymer/nanofiller interactions. The transition from the melt towards the glassy regime is also detected through the sudden increase of "slow" polymer segments, as the temperature decreases, within the model nanocomposites. Last, the significant increase of the average glass transition temperature at high nanoparticle concentrations might be linked to the different types of conformations that the polymer chains adopt when surrounding a nanoparticle. The detailed investigation of the above hypothesis will be the subject of a forthcoming study.

Acknowledgements. This work has received funding from the European Union's Horizon 2020 research and innovation programme under grant agreement No. 810660. This work was also granted access to the HPC cluster Cyclone (Nicosia, Cyprus) in the framework of the projects p060 and p086.

References

1. Bailey, E. J.; Winey, K. I., Dynamics of polymer segments, polymer chains, and nanoparticles in polymer nanocomposite melts: A review. *Prog. Polym. Sci.* **2020,** *105*, 101242.
2. DeFelice, J.; Lipson, J. E. G., The influence of additives on polymer matrix mobility and the glass transition. *Soft Matter* **2021,** *17* (2), 376-387.
3. Papon, A.; Montes, H.; Hanafi, M.; Lequeux, F.; Guy, L.; Saalwächter, K., Glass-Transition Temperature Gradient in Nanocomposites: Evidence from Nuclear Magnetic Resonance and Differential Scanning Calorimetry. *Phys. Rev. Lett.* **2012,** *108* (6), 065702.
4. Randazzo, K.; Bartkiewicz, M.; Graczykowski, B.; Cangialosi, D.; Fytas, G.; Zuo, B.; Priestley, R. D., Direct Visualization and Characterization of Interfacially Adsorbed Polymer atop Nanoparticles and within Nanocomposites. *Macromolecules* **2021,** *54* (21), 10224-10234.
5. Richter, D.; Kruteva, M., Polymer dynamics under confinement. *Soft Matter* **2019,** *15* (37), 7316-7349.

6. Zhang, W.; Emamy, H.; Pazmiño Betancourt, B. A.; Vargas-Lara, F.; Starr, F. W.; Douglas, J. F., The interfacial zone in thin polymer films and around nanoparticles in polymer nanocomposites. *J. Chem. Phys.* **2019,** *151* (12), 124705.
7. Schweizer, K. S.; Simmons, D. S., Progress towards a phenomenological picture and theoretical understanding of glassy dynamics and vitrification near interfaces and under nanoconfinement. *J. Chem. Phys.* **2019,** *151* (24), 240901.
8. Chakraborty, S.; Lim, F. C. H.; Ye, J., Achieving an Optimal Tg Change by Elucidating the Polymer–Nanoparticle Interface: A Molecular Dynamics Simulation Study of the Poly(vinyl alcohol)–Silica Nanocomposite System. *J. of Phys. Chem. C* **2019,** *123* (39), 23995-24006.
9. Fragiadakis, D.; Pissis, P.; Bokobza, L., Glass transition and molecular dynamics in poly(dimethylsiloxane)/silica nanocomposites. *Polymer* **2005,** *46* (16), 6001-6008.
10. Qin, X.; Xia, W.; Sinko, R.; Keten, S., Tuning Glass Transition in Polymer Nanocomposites with Functionalized Cellulose Nanocrystals through Nanoconfinement. *Nano Lett.* **2015,** *15* (10), 6738-6744.
11. Wei, T.; Torkelson, J. M., Molecular Weight Dependence of the Glass Transition Temperature (Tg)-Confinement Effect in Well-Dispersed Poly(2-vinyl pyridine)–Silica Nanocomposites: Comparison of Interfacial Layer Tg and Matrix Tg. *Macromolecules* **2020,** *53* (19), 8725-8736.
12. Montes, H.; Lequeux, F.; Berriot, J., Influence of the Glass Transition Temperature Gradient on the Nonlinear Viscoelastic Behavior in Reinforced Elastomers. *Macromolecules* **2003,** *36* (21), 8107-8118.
13. Berriot, J.; Montes, H.; Lequeux, F.; Long, D.; Sotta, P., Gradient of glass transition temperature in filled elastomers. *Europhys. Lett.* **2003,** *64* (1), 50.
14. Pavlov, A. S.; Khalatur, P. G., Fully atomistic molecular dynamics simulation of nanosilica-filled crosslinked polybutadiene. *Chem. Phys. Lett.* **2016,** *653*, 90-95.
15. Varnik, F.; Binder, K.; Baschnagel, J., Glass transition on thin polymer films: A molecular dynamics study. . *Int. J. Mod. Phys. C* **2002,** *13* (06), 799-804.
16. Varnikl, F.; Scheidlerl, P.; Baschnagel, J.; Kob, W.; Binder, K., Molecular Dynamics Simulation of Confined Glass Forming Liquids. *Mater. Res. Soc. Symp. Pro.* **2000,** *651*, T3.1.1.
17. Peter, S.; Meyer, H.; Baschnagel, J., Thickness-dependent reduction of the glass-transition temperature in thin polymer films with a free surface. *J. Polym. Sci., Part B: Polym. Phys.* **2006,** *44* (20), 2951-2967.
18. Van der Beek, G. P.; Stuart, M. A. C.; Fleer, G. J.; Hofman, J. E., Segmental adsorption energies for polymers on silica and alumina. *Macromolecules* **1991,** *24* (25), 6600-6611.
19. Brown, D.; Mélé, P.; Marceau, S.; Albérola, N. D., A Molecular Dynamics Study of a Model Nanoparticle Embedded in a Polymer Matrix. *Macromolecules* **2003,** *36* (4), 1395-1406.
20. Priestley, R. D.; Cangialosi, D.; Napolitano, S., On the equivalence between the thermodynamic and dynamic measurements of the glass transition in confined polymers. *J. Non. Crys. Solids* **2015,** *407*, 288-295.
21. Fukao, K.; Miyamoto, Y., Glass transition temperature and dynamics of α-process in thin polymer films. *Europhys. Lett.* **1999,** *46* (5), 649.
22. Glomann, T.; Hamm, A.; Allgaier, J.; Hübner, E. G.; Radulescu, A.; Farago, B.; Schneider, G. J., A microscopic view on the large scale chain dynamics in nanocomposites with attractive interactions. *Soft Matter* **2013,** *9* (44), 10559-10571.

23. Glomann, T.; Schneider, G. J.; Allgaier, J.; Radulescu, A.; Lohstroh, W.; Farago, B.; Richter, D., Microscopic Dynamics of Polyethylene Glycol Chains Interacting with Silica Nanoparticles. *Phys. Rev. Lett.* **2013,** *110* (17), 178001.
24. Golitsyn, Y.; Schneider, G. J.; Saalwächter, K., Reduced-mobility layers with high internal mobility in poly(ethylene oxide)–silica nanocomposites. *J. Chem. Phys.* **2017,** *146* (20), 203303.
25. Senses, E.; Darvishi, S.; Tyagi, M. S.; Faraone, A., Entangled Polymer Dynamics in Attractive Nanocomposite Melts. *Macromolecules* **2020,** *53* (12), 4982-4989.
26. Hong, B.; Chremos, A.; Panagiotopoulos, A. Z., Dynamics in coarse-grained models for oligomer-grafted silica nanoparticles. *J. Chem. Phys.* **2012,** *136* (20), 204904.
27. Rissanou, A. N.; Papananou, H.; Petrakis, V. S.; Doxastakis, M.; Andrikopoulos, K. S.; Voyiatzis, G. A.; Chrissopoulou, K.; Harmandaris, V.; Anastasiadis, S. H., Structural and Conformational Properties of Poly(ethylene oxide)/Silica Nanocomposites: Effect of Confinement. *Macromolecules* **2017,** *50* (16), 6273-6284.
28. Skountzos, E. N.; Karadima, K. S.; Mavrantzas, V. G. Structure and Dynamics of Highly Attractive Polymer Nanocomposites in the Semi-Dilute Regime: The Role of Interfacial Domains and Bridging Chains. *Polymers* **2021**, *13* (16), 2749.
29. Skountzos, E. N.; Tsalikis, D. G.; Stephanou, P. S.; Mavrantzas, V. G., Individual Contributions of Adsorbed and Free Chains to Microscopic Dynamics of Unentangled poly(ethylene Glycol)/Silica Nanocomposite Melts and the Important Role of End Groups: Theory and Simulation. *Macromolecules* **2021,** *54* (10), 4470-4487.
30. Hess, B.; Kutzner, C.; van der Spoel, D.; Lindahl, E., GROMACS 4: Algorithms for Highly Efficient, Load-Balanced, and Scalable Molecular Simulation. *J. Chem. Theory Comput.* **2008,** *4* (3), 435-447.
31. Power, A. J.; Papananou, H.; Rissanou, A. N.; Labardi, M.; Chrissopoulou, K.; Harmandaris, V.; Anastasiadis, S. H., Dynamics of Polymer Chains in Poly(ethylene oxide)/Silica Nanocomposites via a Combined Computational and Experimental Approach. *J. Phys. Chem. B* **2022,** *126* (39), 7745-7760.
32. Harmandaris, V.; Floudas, G.; Kremer, K.; Dynamic heterogeneity in fully miscible blends of polystyrene with oligostyrene, *Phys. Rev. Let.* **2013**, *110*, 165701.
33. Colmenero, J.; Arbe, A., Recent progress on polymer dynamics by neutron scattering: From simple polymers to complex materials. *J. Polym. Sci., Part B: Polym. Phys.* **2013,** *51* (2), 87-113.
34. Frick, B.; Richter, D.; Petry, W.; Buchenau, U., Study of the glass transition order parameter in amorphous polybutadiene by incoherent neutron scattering. *Z. Phys. B Con. Mat.* **1988,** *70* (1), 73-79.
35. Richter, D.; Monkenbusch, M.; Arbe, A.; Colmenero, J., Neutron scattering and the glass transition in polymers – present status and future opportunities. *Journal of Non-Crystalline Solids* **2001,** *287* (1), 286-296.
36. Starr, F. W.; Douglas, J. F.; Sastry, S., The relationship of dynamical heterogeneity to the Adam-Gibbs and random first-order transition theories of glass formation. *J. Chem. Phys.* **2013,** *138* (12), 12A541.
37. Lyulin, A. V.; Michels, M. A. J., Molecular Dynamics Simulation of Bulk Atactic Polystyrene in the Vicinity of Tg. *Macromolecules* **2002,** *35* (4), 1463-1472.
38. Pazmiño Betancourt, B. A.; Douglas, J. F.; Starr, F. W., String model for the dynamics of glass-forming liquids. *J. Chem. Phys.* **2014,** *140* (20), 204509.
39. Elmahdy, M. M.; Chrissopoulou, K.; Afratis, A.; Floudas, G.; Anastasiadis, S. H., Effect of Confinement on Polymer Segmental Motion and Ion Mobility in PEO/Layered Silicate Nanocomposites. *Macromolecules* **2006,** *39* (16), 5170-5173.

40. Tanis, I.; Tragoudaras, D.; Karatasos, K.; Anastasiadis, S. H., Molecular Dynamics Simulations of a Hyperbranched Poly(ester amide): Statics, Dynamics, and Hydrogen Bonding. *J. Phys. Chem. B* **2009,** *113* (16), 5356-5368.
41. Reda, H.; Chazirakis, A.; Behbahani, A. F.; Savva, N.; Harmandaris, V., Mechanical properties of glassy polymer nanocomposites via atomistic and continuum models: The role of interphases. *Comput. Methods Appl. Mech. Eng.* **2022,** *395*, 114905.
42. Bailey, E. J.; Tyagi, M.; Winey, K. I., Correlation between backbone and pyridine dynamics in poly(2-vinyl pyridine)/silica polymer nanocomposites. *J. Polym. Sci.* **2020,** *58* (20), 2906-2913.
43. Chai, Y.; Salez, T.; McGraw, J. D.; Benzaquen, M.; Dalnoki-Veress, K.; Raphaël, E.; Forrest, J. A., A Direct Quantitative Measure of Surface Mobility in a Glassy Polymer. *Science* **2014,** *343* (6174), 994-999.
44. Tanis, I.; Karatasos, K.; Salez, T., Molecular Dynamics Simulation of the Capillary Leveling of a Glass-Forming Liquid. *J. Phys. Chem. B* **2019,** *123* (40), 8543-8549.
45. Napolitano, S.; Lupaşcu, V.; Wübbenhorst, M., Temperature Dependence of the Deviations from Bulk Behavior in Ultrathin Polymer Films. *Macromolecules* **2008,** *41* (4), 1061-1063.
46. Song, Z.; Rodríguez-Tinoco, C.; Mathew, A.; Napolitano, S., Fast equilibration mechanisms in disordered materials mediated by slow liquid dynamics. *Sci. Adv.* **2022**, *8* (15), 7154.
47. Debot, A.; White, R. P.; Lipson, J. E. G.; Napolitano, S., Experimental Test of the Cooperative Free Volume Rate Model under 1D Confinement: The Interplay of Free Volume, Temperature, and Polymer Film Thickness in Driving Segmental Mobility. *ACS Macro Lett.* **2019,** *8* (1), 41-45.
48. White, R. P.; Lipson, J. E. G., To Understand Film Dynamics Look to the Bulk. *Phys. Rev. Lett.* **2020,** *125* (5), 058002.